EXTENDED LENS MODEL CALIBRATION OF DIGITAL STILL CAMERAS

Mark R. Shortis

Department of Geomatics
University of Melbourne
Parkville 3052
AUSTRALIA
M.Shortis@unimelb.edu.au

Stuart Robson

Department of Geomatic Engineering
University College London,
London WC1E 6BT
ENGLAND
S.Robson@ge.ucl.ac.uk

Horst A. Beyer

Imetric SA
Technolpole
CH-2900 Porrentruy
SWITZERLAND
imetric@dial.eunet.ch

ISPRS Commission V Working Group V/1 : Close Range Imaging and Metrology

KEY WORDS : Digital still camera, calibration, lens distortion, depth of field variation, calibration model

ABSTRACT

Digital still cameras have been widely adopted for close range photogrammetry and machine vision applications. Due to the advantages of on board storage of digital images, portability and rapid data processing, digital still cameras have virtually replaced medium format film cameras for measurement tasks such as structural monitoring and industrial metrology. As for any photogrammetric application, the accuracy of the derived object data is dependent on the accuracy of the camera calibration, amongst many other factors. For photogrammetric applications in which accuracy is not of paramount importance or the object is larger than a few metres in size, use of a simple model of lens distortion in conjunction with the collinearity equations is sufficient. However, the combination of very close ranges and the large distortions typically associated with the lenses used with digital still cameras requires an extended lens model to account for variation of distortion within the object space. The fidelity of the calibration model becomes particularly important where stringent tolerances are set, for example in aerospace inspection tasks. This paper reviews previous research into distortion variation and outlines an investigation of the modelling of this systematic error. The calibration procedure, utilising a straight line calibration range, is described. Experimental results for Kodak DCS420 and DCS460 digital still cameras, including an assessment of the effect and repeatability of the distortion variation, are presented.

1. INTRODUCTION

Close range photogrammetry has rapidly embraced the new technology of digital still cameras because they are portable and reliable, and have the added advantages of automated image measurement and rapid data processing (Fraser and Shortis, 1995). Reported videometric applications of these cameras include architectural recording, low altitude mapping, large scale engineering metrology and tool inspection for the aerospace industry (Beyer, 1995). High resolution digital still cameras such as the Kodak DCS460 and Rollei Q16 are capable of relative precisions of the order of 1:300,000 (Peipe, 1997; Shortis *et al.*, 1998), assuming a suitable target image location algorithm and a self-calibrating network of many camera stations.

High resolution digital still cameras have not yet realised their full potential because the discrepancy between the theoretical and actual accuracy is wider than the discussion above would suggest. Whilst internal precisions of 0.02 pixels are routinely reported, independent checking of photogrammetric networks utilising still video cameras indicates that the internal precision is not always a reliable indicator of external accuracy (Fraser and Shortis, 1995; Shortis *et al.*, 1995; Shortis *et al.*, 1998). Relatively few applications have incorporated an independent measurement of the target object space coordinates, generally supplied using film cameras, theodolite systems or coordinate measuring machines. Although there is always an element of doubt associated with such comparisons due to the implicit assumptions of object stability and consistency of target location measurement, many independent tests have indicated a significantly degraded external accuracy when compared to internal precision.

Clearly, systematic or stochastic errors remain in the model for the optical and electronic components of digital still cameras or the target location algorithms for image measurement. Because there are many possible sources of error, the best approach to the problem is one of elimination. One area of valid research is the common use of a simple lens model which assumes radial lens distortions are constant with respect to the distance between the lens and the target. This paper will concentrate on initial research toward the evaluation of an extended lens model which incorporates variation of radial lens distortion within the depth of field.

2. LENS DISTORTION VARIATION

An image is considered to be in focus at a specific distance, known as the focus setting or focus distance for the camera lens. The plane of best focus in the object field is a plane parallel to the image plane. It is well known that lens distortion varies with lens focus. A change in the focus distance for a typical camera with a simple lens system is achieved by a change in the principal distance, which changes the image magnification produced by the camera lens. The change in the principal distance results in a change in lens distortion which is proportional to the principal distance and the focus distance.

Magill (1955) developed a formula for the computation of lens distortion at any specified focus distance, or magnification, based on two other determinations of lens distortion profiles. The formula, with some minor modifications, has been verified experimentally for both radial and decentring lens distortion for conventional film cameras (Brown, 1971; Fryer and Brown, 1986) and, more recently, with video and digital still cameras (Fryer and Mason, 1989; Wiley and Wong, 1995)

However, the formula is rarely used in practice, as it is typical that photogrammetric applications use cameras at a single focus setting. If the lens is focussable, it is often taped or otherwise fixed in place so that no change in focus is possible. The rationale for this strategy is based on the limitations of any theoretical formula and the widespread use of self-calibrating bundle solutions. In essence, no matter how well the formula models the change in lens distortion with focus, a more reliable solution will be obtained with self-calibration of a single, block-invariant set of calibration parameters. If multiple focus settings are required, then the parameters are better modelled by multiple calibration sets which effectively treat the different focus settings of the same camera as if they were different cameras (Shortis *et al.*, 1996).

Simple lens distortion models, derived from a calibration or the application of Magill's formula are applicable only to the plane of best focus. If the intent is to image an approximately planar object with near orthogonal imagery, then the simple lens distortion model is sufficient. However, lens distortion does vary within the object space, although the magnitude of the variation is typically much less than the variation with focus distance (Fraser and Shortis, 1992). The variation increases with magnification and distance from the plane of best focus, and so this effect is certainly relevant to close range photogrammetric and machine vision applications where the object to be measured extends across a significant range in the object space. In particular, applications which require high accuracy, such as tool inspection and surface characterisation for the aerospace and manufacturing industries, require an extended lens model to eliminate the systematic error caused by variation within the depth of field (Fraser and Shortis, 1992).

Brown (1971) developed an extended lens model to account for the variation of distortion outside of the plane of best focus. The model is based on a function of the lens distortion at the plane of best focus and a scale factor derived from the geometry of the image :

$$\delta r_{ss'} = \frac{1}{\gamma_{ss'}} \delta r_{s'} \qquad (1)$$

where

$\delta r_{ss'}$ = radial distortion at an object distance s' for a lens focussed at an object distance s

$\delta r_{s'}$ = radial distortion at an object distance s' for a lens focussed at an object distance s'

s = focus distance for the camera

s' = distance to the plane of the target point

The scale factor is given by :

$$\gamma_{ss'} = \frac{c_{s'}}{c_s} = \frac{s'}{s} \cdot \frac{(s - f)}{(s' - f)} \qquad (2)$$

where

c_s = principal distance for the focus distance s

$c_{s'}$ = principal distance for the focus distance s'

Brown demonstrated that this formulation is applicable to lenses with a moderate distortion profile, but it is evident that the scale factor must always be positive and the function cannot model all variations in distortion across the depth of field. Fraser and Shortis (1992) subsequently showed that the extended model developed by Brown is not able to model the variations in distortion when the magnitude of the distortion, and therefore the gradient of distortion across the format, is very large or if the distortion magnitudes are not increasing with decreasing magnification. An alternative model was developed which expresses the lens distortion as a function of the distortions at the distances of the camera focus and the point of interest :

$$\delta r_{ss'} = \delta r_s + g_{ss'} (\delta r_{s'} - \delta r_s) \qquad (3)$$

where

$g_{ss'}$ = a constant value derived empirically

δr_s = radial distortion at an object distance s for a lens focussed at an object distance s

Fraser and Shortis (1992) verified this new extended lens model for large and medium format film cameras, and showed that the significance of the correction is greater at close camera to object distances. The lens to lens variation was relatively low, although clearly present. Hence the empirically derived constant factor $g_{ss'}$ could be applied to any lens of a specific type and the model error was shown to be significantly less than the magnitude of the distortion variation. The advantage of this model is that it can accurately represent a wide range of distortions profiles, however the disadvantage is that distortion profiles must be determined at a sufficient number of focus settings to cover the desired depth of field.

3. LENS DISTORTION CALIBRATION

3.1 Calibration Technique

In order to test a number of extended lens models for typical digital still cameras, an experiment was designed to conduct a comprehensive camera calibration and accuracy test. The basis for the calibration was a test range constructed at Imetric SA to enable the simultaneous targeted test range and straight line calibration of Kodak DCS420 and DCS460 digital still cameras. The calibration range comprises 20 vertical white plastic strands under tension, mounted in front of a black back board. There are 80 retro-reflective targets on the back board, and with the addition of approximately 65 targets on carbon fibre rods placed in the foreground, the calibration range provides a suitably dense, three dimensional array of points. An image of the test range is shown in figure 1.

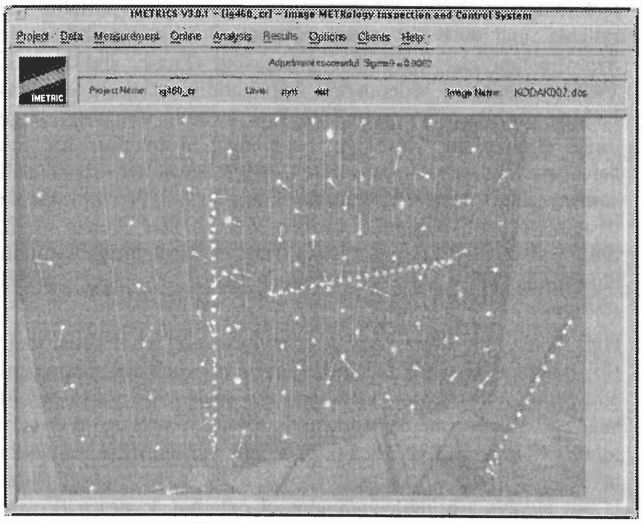

Figure 1. Calibration range image.

Shortis *et al.* (1995) showed that the combination of target array and straight line calibrations realises calibration parameters with optimum accuracy and independence. Calibration using a target array, multiple convergent images and a self-calibrating solution can determine all parameters very precisely, but does not obtain all parameters with a high degree of independence. Strong correlations, for example between principal point and decentring distortion parameters, are common despite the very large numerical redundancy of networks comprising many targets and many images. Calibration using straight lines can determine only the lens distortions, albeit with a high level of independence and accuracy, however knowledge of all calibration parameters is required for a complete calibration parameter set and the successful integration of the two techniques.

In accord with common practice, the cameras are set to an initial focus and the lens locked by taping the focus barrel to the lens barrel. Due to the very short focal length lenses used to obtain an acceptable field of view for digital still cameras, the most convenient focus setting is infinity. Setting infinity focus is repeatable, as the focus barrel is at the end of its run, and provides a depth of field from infinity to as close as 0.5 metres, depending on the lens. This depth of field is more than adequate for most industrial applications.

The self-calibrating network solutions comprised 24 or 32 images using six or eight camera stations of convergent photography and four exposures at each station, adopting the usual orthogonal roll strategy used in industrial metrology for minimisation of parameter correlations. The network solutions used a mixture of block-invariant and photo-invariant parameters, in order to accommodate the known CCD array movement in the Kodak DCS camera series (Shortis *et al.*, 1998).

The straight line image sets consisted of six to nine stations at distances ranging from approximately 0.6 to 2.9 metres from the straight lines. At each station, multiple exposures were taken, again by rolling the camera. In the case of straight line calibrations, this strategy is required to strengthen the calibration with more data points on the straight lines throughout the image format, and to fully determine the decentring distortion parameters. Additional rolled exposures were taken at the nearest stations to the straight lines to further densify the data across the image format. This was particularly important as despite increasing the density of lines toward the centre of the field, the proximity of the camera to the test range reduces the number of visible straight lines (figure 1). Within the range of distances for the straight line exposures, the mid-range stations tend to realise the most precise and accurate results. At the near distances the line density is low, whilst at the far focus distance the straight lines cover only the central 50% of the image format, reducing the effectiveness of the calibrations. Data sets closer than 0.6m were not viable, due a combination of high levels of measurement uncertainty attributable to the very large width of the straight lines in the images, and the sparseness of the data due to the large line spacing in the images.

Camera	Focal Length (mm)	Stations	Range (m)	Number of Images	Number of Line Points
DCS420	14mm	6	0.60-2.80	25	5800
DCS420	18mm	6	1.08-2.88	18	4100
DCS460 #1	18mm	6	0.72-2.16	20	3900
DCS460 #1	20mm	6	0.80-2.80	20	4000
DCS460 #2	20mm	9	0.60-2.80	27	7400
DCS460 #1	24mm	6	0.96-2.64	20	3800

Table 1. Details of straight line calibration tests.

Great care was taken to ensure that the distances matched specific magnifications for each lens and the image plane was parallel to the plane of the straight lines. This in effect produces particular "slices" through the depth of field for the camera lens, which can then be modelled in terms of the variation in the lens distortion. Details of the straight line calibration sets are given in table 1. The data was captured using a Kodak DCS420, two DCS460s and six different 35mm SLR lenses.

3.2 Calibration Results

The straight line calibrations are partially based on the targeted test range and network solutions, as non-distortion calibration parameters such as the principal point location are required for the straight line calibrations. The straight line calibrations for each "slice" through the depth of field are then separately processed to provide a precise and independent estimate of the lens distortions at each distance. Because the camera and lens are unaltered, other than perhaps by handling (Shortis and Beyer, 1997), it can be assumed that calibration parameters such as the principal distance do not change during the entire procedure. It has been shown that the principal point location does apparently move (Shortis *et al.*, 1998), due to the movement of the CCD array in response to different roll angles, but the magnitude of the movement is generally no greater than 60 microns and would have little effect on the computation of the lens distortion magnitudes. For example, a shift in the principal point location by 30 microns in x and y for the second DCS460 with the 20mm lens results in a change in the radial lens distortion profile of only 0.02 microns at a radius of 12mm. The change in the decentring lens distortion profile of 0.4 microns is much more significant, however this is a worst case scenario and it could be expected that any effect would tend to be averaged across the multiple images contributing the straight line calibration.

Shown in table 2 are indicative results of the straight line calibrations. The range of RMS image residuals and magnitudes of the radial and decentring lens distortion profiles are shown for the extremes of the station locations for each case. The RMS image residuals show a consistent trend of higher residuals at closer distances to the straight lines. This trend is readily explained considering the previous discussions of the problems of very close range images and the decreasing format coverage of the more distant images.

Camera	Focal Length (mm)	Range (m)	RMS Image Resid. (μm)	Max and Min Lens Distortion (μm)	
				Radial	Decent.
DCS420	14mm	0.70	0.80	85.9	2.8
		2.80	0.26	80.3	1.7
DCS420	18mm	1.44	1.04	47.8	2.9
		2.88	0.56	46.5	1.5
DCS460	18mm	0.72	1.25	290.9	5.7
		2.16	0.49	284.5	5.6
DCS460	20mm	0.80	1.02	297.6	1.1
		2.80	0.41	291.1	0.6
DCS460	20mm	0.60	2.04	341.1	2.3
		2.80	0.52	330.8	3.3
DCS460	24mm	0.96	1.18	271.8	1.8
		2.64	0.51	267.8	0.8

Table 2. Results of straight line calibration tests (lens distortion profile values are computed at 6mm and 12mm radius for the DCS420 and DCS460 camera respectively).

Table 2 shows clearly that there is a small but significant signal from the changing range between the camera and the straight line calibration field, and therefore it can be deduced that there is significant variation in distortion within the depth of field for these types of camera lens. Similar results were obtained in earlier experiments at the University of Melbourne using a DCS420 camera (Shortis *et al.*, 1996). Secondly, in all cases for the radial distortion, the magnitude of the distortion generally decreases as the position within the depth of field approaches the focus distance. In other words, at the extreme edge of the depth of field away from the camera, the radial distortion is smallest in magnitude. Note that all of these lenses exhibit barrel distortion, which by convention is negative. The decentring distortion is less consistent, with some lenses showing no change and one lens exhibiting an increase in distortion magnitude, contrary to the general trend. Decentring is attributable to mechanical misalignment of individual lens elements and could be expected to be inconsistent between lenses.

4. ANALYSIS OF THE CALIBRATION RESULTS

Given that the signal from the radial lens distortion, whilst quite small, is considerably greater than signal from the decentring distortion, the following analysis will concentrate on the radial lens distortion. A similar approach was adopted by Fraser and Shortis (1992) because the signal from the variation in decentring distortion was barely significant.

4.1 Distortion Profiles

The change in radial lens distortion within the depth of field is not a linear progression, as is shown in figure 2. This graph shows the variation in radial lens distortion magnitude plotted against magnification in order to give a common scale for all six lenses. Differences are computed relative to the distortions at the maximum camera to object distance, as this most closely corresponds to the actual distortion profile at infinity focus.

At higher magnifications the changes in distortion are approximately linear, but at smaller magnifications, or closer distances to the object within the depth of field, the distortion changes are distinctly non-linear. A number of the lenses show a peak in distortion change at around 50 to 75 times magnification. The similar behaviour of the two 20mm lenses and the disparate behaviour of the two 18mm lenses may be due to the design and construction of the lenses. The two 20mm lenses and the 18mm lens used with the DCS460 were from the same manufacturer, whilst the 18mm lens used with the DCS420 was from a different manufacturer.

Figure 2 shows only the change at a single point on the radial lens distortion profile. In figure 3, the change in the radial lens distortion profiles is shown for the case of the DCS460 with the 20mm lens. This set of profiles shows typical behaviour in the sense that there is a general increase in the change in radial distortion with decrease in magnification. In this case there appears to be a grouping of curves for the range of 40 to 60 times magnification, indicating that the change in distortion within the depth of field has reached a peak at around 50 times magnification. Only the second DCS460, used with a 20mm lens, does not show a peak in the curve. Once more, a decrease in magnification is equivalent to objects closer to the camera within the depth of field.

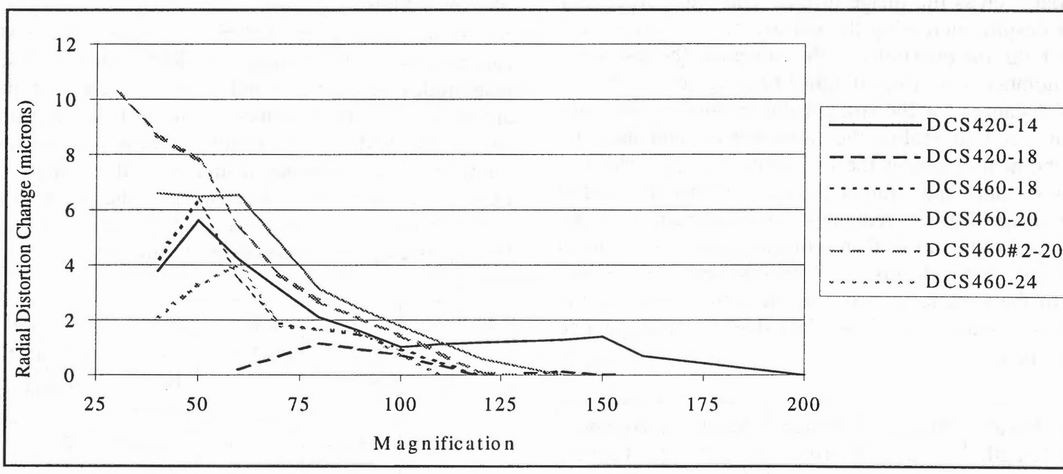

Figure 2. Change in radial lens distortion for the six lenses.

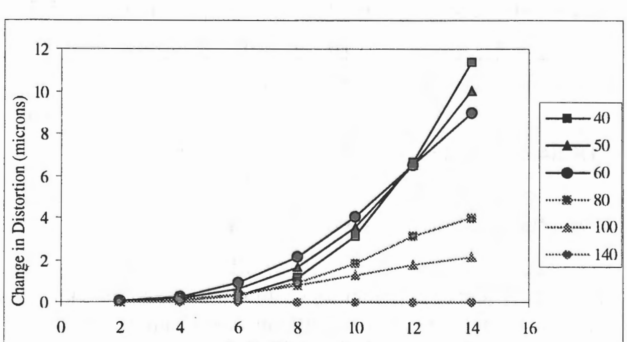

Figure 3. Change in the radial lens distortion profiles with magnification for the DCS460 with the 20mm lens.

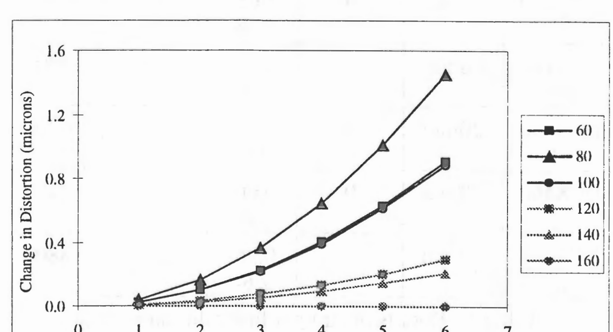

Figure 4. Change in the decentring lens distortion profiles with magnification for the DCS420 with the 18mm lens.

The decentring component of the lens distortion generally shows a more erratic behaviour, as could be predicted from the data presented in table 2. The example given in figure 4 shows a similar pattern to the radial distortion in figure 3, but this is a good example of the variation in the decentring distortion.

4.2 Variation Model

The previous discussions have established that the models developed for lens distortion variation within the depth of field of a camera by Brown (1971) and Fraser and Shortis (1992) cannot be readily employed for industrial inspection applications. Brown's model is inadequate for data sets such as these where there is a clear discontinuity in the trend. The data collection for the Fraser and Shortis implementation is demanding and the full functional model is not readily integrated into a self-calibrating network solution where the distortion functions are based on a local additional parameter model.

However, as was indicated in Fraser and Shortis (1992), once the gradient of the distortion change was established for a particular lens type, it could be applied to many lenses of that type with a relatively small error. A gradient factor is a straightforward extension to the additional parameter model, based on the lens distortions derived from the self-calibrating solution. In the case of the large format film cameras used by Fraser and Shortis, the gradient function is applied to the computed distortions at locations outside of the plane of best focus.

A similar strategy is adopted here as a first stage of developing a functional model, primarily because this model can be readily implemented in a self-calibrating network solution. In the case of the digital still cameras, the gradient function is applied to all object locations assuming the camera is focussed at infinity. To enable a straightforward numerical implementation, the gradient correction in a plane parallel to the image plane of the exposure can be applied as a factor which is inversely proportional to the denominator of the collinearity equations.

A gradient model which incorporates the inflection points shown in figure 2 would be a complex function. Given the profiles shown in figure 2, the assumption was made that the majority of target points will be within the range of 40 and higher magnifications. Object locations at magnifications of less than 40 times must be at a range of less than approximately 0.8 metres from the camera. Whilst this is certainly possible, it is likely that in a situation where the majority of targeted points were at this distance the camera would be re-focussed at an appropriate, non-infinity setting.

Camera	Focal Length (mm)	Gradient Factor		RMS Error (μm)	
		Radial (10^3)	Decent.	Radial	Decent.
DCS420	14mm	25	250	0.5	0.2
DCS420	18mm	11.5	300	0.9	0.5
DCS460	18mm	9	0	1.1	0.1
DCS460	20mm	20	600	1.1	0.1
DCS460	20mm	20	-150	0.7	0.1
DCS460	24mm	15	700	1.0	0.2

Table 3. Gradients of lens distortion change.

The gradients of distortion change for each of the lenses can be computed by curves of best fit to the change in distortion for all points on the radial and decentring lens distortion profiles, ignoring data at magnifications less than the inflection points for the curves shown in figure 2. As the graph for the second DCS460 with the 20mm lens shows no inflection point, the entire data series was used. Using an empirical regression analysis, it was found that the optimum function for the change in radial lens distortion was a second order curve, whereas due to the small signal the decentring lens distortion was adequately modelled by a simple linear function. Hence the change in distortion within the depth of field of the camera is inversely proportional to the square of the distance and the distance only for the radial and decentring distortions respectively.

The gradients computed using these functions are shown in table 3. The factors for radial distortion are consistent and there is good agreement between lenses with similar focal lengths. The factors for the decentring distortion are, as again could be expected from the low and erratic signal, somewhat inconsistent. Also shown in the table are the RMS errors between the measured and computed profiles within the depth of field for each camera and lens combination. In most cases these errors are comparable to the RMS measurement errors for the straight line images. With the exception of the DCS420 and 18mm lens, the level of error for the lens distortions is approximately 20% of the signal. Hence for all other cases the use of the distortion gradients within the depth of field could be expected to improve a self-calibrating network solution.

5. NETWORK VERIFICATION

To test the efficacy of the distortion gradients, network adjustments for the targeted test range calibrations were re-computed with the incorporation of the gradients. The results for the networks with and without the gradient functions are shown in table 4, along with the characteristics of each network. The key indicator in table 4 is the estimate of unit weight for the networks, also known as sigma zero, which is based on *a priori* image measurement precisions provided by least squares template matching of the retro-reflective target images.

Camera	Focal Length (mm)	Targets	Images	Estimate of Unit Weight	
				Simple Model	Gradient Model
DCS420	14mm	90	24	0.92	0.89
DCS420	18mm	110	24	0.85	0.85
DCS460	18mm	160	32	1.07	1.06
DCS460	20mm	160	32	1.11	1.10
DCS460	20mm	145	24	1.11	1.09
DCS460	24mm	140	24	0.83	0.82

Table 4. Results of targeted test range calibration tests with and without the gradient function for change in distortion.

It is clear from the results for the estimate of unit weight that there is only a very small improvement in the internal consistency for five of the photogrammetric networks. As expected, there is no improvement at all for the DCS420 with the 18mm lens.

The improvement for some of the networks may be statistically significant, as the numerical redundancy for the DCS460 networks is of the order of 8000. However, the gradient functions clearly have little effect and there is no significant improvement in practical terms. Further experimental testing is required to determine whether the gradient functions have any impact on external accuracy.

6. CONCLUSIONS

This paper has demonstrated that there is a significant variation in the magnitude of lens distortions within the depth of field of typical 35mm SLR type lenses used with the Kodak DCS420 and DCS460 cameras. The specific case of the lens focussed at infinity has been investigated to accord with common use of these cameras for industrial inspection.

Gradient function models for the radial and decentring distortion variations have been tested as a method of conveniently introducing the variation into self-calibrating network solutions. The gradient functions are valid only for high magnifications and although the models adequately represent the signal of the variation, there remains some substantive discrepancies between the theoretical functions and the measured profiles of distortion variation. As a consequence, the introduction of the gradient functions realises only minor improvements in the internal consistency of the networks

There is no doubt that the initial functional model is incomplete. A substantial amount of further data collection, analysis and validation is required to establish a more comprehensive functional model for the variation of distortion within the depth of field. Whereas the inclusion of the inflection points in the model may be impractical, the nature of these peaks in the change in distortion needs to be verified. In addition, the effect of the inclusion of the extended lens model on external accuracy, as well as internal network consistency, is necessary. Finally, the applicability of this approach to focus settings other than infinity, and the effect of the movement of the principal point location for the DCS camera series, are also worthy of investigation.

A complete and accurate functional model of the variation of distortion has the potential to improve both the internal consistency and the external accuracy of close range self-calibrating networks. The model should be particularly effective for industrial inspection networks which involve short focal length lenses and large depths of field. The practical advantages of this approach are that the model does not weaken the adjustment process by over-parameterisation and the gradient function can be readily implemented in a network solution.

REFERENCES

Beyer, H. A., 1995. Digital photogrammetry in industrial applications. *Int. Arch. of Photogrammetry and Remote Sensing*, 30(5W1) : 373-375.

Brown, D. C., 1971. Close-range camera calibration, *Photogrammetric Engineering*, 37(8) : 855-866.

Fraser, C. S. and Shortis, M. R., 1992. Variation of distortion within the photographic field. *Photogrammetric Engineering and Remote Sensing*, 58(6) : 851-855.

Fraser, C. S. and Shortis, M. R., 1995. Metric exploitation of still video imagery. *Photogrammetric Record*, 15(85) : 107-122.

Fryer, J. G. and Brown, D. C., 1986. Lens distortion for close-range photogrammetry, *Photogrammetric Engineering and Remote Sensing*, 52(1) : 51-58.

Fryer, J. G. and Mason, S. O., 1989. Rapid lens calibration of a video camera. *Photogrammetric Engineering and Remote Sensing*, 55(4) : 437-442.

Magill, A. A., 1955. Variation in distortion with magnification. *Journal of Research of the National Bureau of Standards*, 54(3) : 153-142.

Peipe, J., 1997. High-resolution CCD area array sensors in digital close range photogrammetry. *Videometrics V*, SPIE Vol. 3174, pp 153-156.

Shortis, M. R. and Beyer, H. A, 1997. Calibration stability of the Kodak DCS420 and 460 cameras. *Videometrics V*, SPIE Vol. 3174, pp 94-105.

Shortis, M. R., Robson, S. and Beyer, H. A., 1998. Principal point behaviour and calibration parameter models for Kodak DCS cameras. Submitted to *Photogrammetric Record.*

Shortis, M. R., Robson, S. and Short, T., 1996. Multiple focus calibration of a still video camera. *Int. Arch. of Photogrammetry and Remote Sensing,* 31(B5) : 534-539.

Shortis, M. R., Snow, W. L. and Goad, W. K., 1995. Comparative geometric tests of industrial and scientific CCD cameras using plumb line and test range calibrations. *Int. Arch. of Photogrammetry and Remote Sensing*, 30(5W1) : 53-59.

Wiley, A. G. and Wong, K. W., 1995. Geometric calibration of zoom lenses for computer vision metrology. *Photogrammetric Engineering and Remote Sensing*, 61(1) : 69-74.